Applied Clay Science

Volumes 132–133, November 2016, Pages 167–174

http://dx.doi.org/10.1016/j.clay.2016.06.001

http://www.sciencedirect.com/science/article/pii/S016913171630237X

# ADSORPTION OF AN ACTIVE MOLECULE ON THE SURFACE OF HALLOYSITE FOR CONTROLLED RELEASE APPLICATION: INTERACTION, ORIENTATION, CONSEQUENCES

József Hári[1,2], Péter Polyák[1,2], Dávid Mester[1,3], Matej Mičušík[4], Mária Omastová[4], Mihály Kállay[1,3], Béla Pukánszky[1,2]

[1]Department of Physical Chemistry and Materials Science, Budapest University of Technology and Economics, H-1521 Budapest, P.O.Box 91, Hungary

[2]Institute of Materials and Environmental Chemistry, Research Centre for Natural Sciences, Hungarian Academy of Sciences, H-1519 Budapest, P.O. Box 286, Hungary

[3]MTA-BME Lendület Quantum Chemistry Research Group, Department of Physical Chemistry and Materials Science, Budapest University of Technology and Economics, P.O. Box 91, Budapest 1521, Hungary

[4]Polymer Institute, Slovak Academy of Sciences, Dúbravská cesta 9, 845 41 Bratislava 45, Slovak Republic

*Corresponding author: Phone: +36-1-463-4078, Fax: +36-1-463-3474, Email: jhari@mail.bme.hu

**Abstract**

The goal of the study was to check the possible use of halloysite nanotubes as a controlled release natural antioxidant device with quercetin as the active component. The mineral was thoroughly characterized by various techniques including the determination of particle and tube morphology, specific surface area, pore size and volume, as well as surface energy. The high surface energy of halloysite predicted strong adsorption of active molecules on its surface and consequently difficult release. FTIR spectroscopy confirmed the existence of strong interactions, energetically heterogeneous halloysite surface and multilayer coverage at large loadings. FTIR and XRD experiments proved the complete lack of intercalation and showed that below 3.5 wt% quercetin loading, most of the molecules are located within the halloysite tubes. Molecular modelling indicated the parallel orientation of quercetin molecules with the surface. Critical concentrations derived from various measurements agreed well with each other further confirming that up to about 4.0 wt% loading, quercetin is bonded very strongly to the halloysite surface. As a consequence, the dissolution of active molecules is very difficult or impossible, especially into apolar media, thus neither stabilization nor controlled release effect can be expected below that concentration.

## 1. Introduction

Active molecules are often loaded onto carrier materials for various reasons. Supports may help homogeneous distribution in a matrix or occasionally they may provide a controlled release function as well. Controlled release is increasingly important in many fields of applications, mainly in drug delivery, but also in other areas. A wide variety of nanomaterials are used to achieve the controlled release function. Cyclodextrin, a cyclic oligosaccharide containing a number of hydrogen donor and acceptor groups and an internal

lipophobic surface, can host various molecules in its cavity and is frequently used in delivery systems [1]. Various natural and synthetic polymers like liposomes, polymer micelles, nanoparticles and nanogels are available as controlled release carriers, but porous nanoparticles and various nanofillers with tubular structure are also often used as supports in such applications.

Besides titanium dioxide and carbon nanotubes, halloysite nanotubes are also good potential carriers for active molecules, and were claimed to offer controlled release function as well [2-15]. As a consequence, numerous attempts were made to use them for controlled drug delivery, but also in other applications. Shchuckin et al. [3], for example, developed a corrosion inhibitor coating in which the inhibitor was placed inside halloysite nanotubes and the release of the active component occurred in a controlled way. Liu and Zhao [16] achieved catalytic action by the adsorption of silver nanoparticles onto the surface of halloysite, while Xie [17] prepared magnetic nanotubes in a similar way. The large and high energy surface of halloysite is frequently used also to bind various molecules, especially in water treatment and purification [18, 19]. Most of these applications require a detailed knowledge of halloysite morphology and surface properties, but the mineral is rarely characterized in detail. Particle characteristics, surface area, pore size and volume, as well as surface energy are rarely determined, although they must influence both the adsorption and release of active molecules.

Polyolefins, including polyethylene (PE), usually contain a phenolic antioxidant to provide both processing and long term stability. Although the type and amount of the stabilizer may vary with the application area, its presence is practically inevitable. Unfortunately, approximately a decade ago, concerns arose about the possible health hazard of using synthetic phenolic antioxidants [20], but no viable substitute has been found yet. Nature supplies a number of compounds with considerable antioxidant effect, vitamin E

being the best known representative used also in practice [21-24]. Quercetin is a natural flavonoid with proven antioxidant, antiviral and anti-inflammatory effect which also proved to be a very efficient stabilizer in PE [25]. However, besides its advantages, the compound has several drawbacks as well. Its melting temperature is around 320 °C, well above the processing temperature of PE, its solubility in the polymer is very small and it gives PE a very strong yellow color. Using a solid support to distribute quercetin in PE may improve homogeneity considerably. Halloysite seemed to be an obvious choice as carrier material and possible controlled release effect could be an additional bonus. However, the adsorption and release of an active molecule from the surface depends on a large number of factors including the characteristics of the halloysite and those of the surrounding medium.

Accordingly, the goal of our study was to characterize the halloysite used as thoroughly as possible, determine its interactions with the active molecule and identify the location of this latter on or inside the filler, if possible. We wanted to determine the amount of adsorbed quercetin, as well as the kinetics of adsorption. Preliminary calculations and modelling were carried out to estimate the arrangement of quercetin molecules on the surface of the mineral and to predict possible consequences.

## 2. Experimental

The quercetin used in the study was obtained from Sigma-Aldrich, USA and used as received. Its molecular weight is 302,24 g/mol, melting temperature 316 °C and purity >95 %. The molecular structure of quercetin is presented in **Scheme 1**. The halloysite used in the experiments was obtained from Applied Minerals (USA). Its particle size was determined in ethanol suspension after sonication for 60 min using a Horiba Partica LA950V2 particle size analyzer. Particle characteristics were also determined by the image analysis of transmission electron micrographs (TEM) recorded with the help of a FEI

Morgagni 268D apparatus. Average values of external and internal diameter as well as the length of the tubes were derived from the measurement of more than 70 individual tubes. Specific surface area, pore size and volume were measured using a NOVA 2000 (Quantachrome, USA) apparatus. The measurements were done at -195 °C after evacuating the sample at 120 °C for 24 hours down to $10^{-5}$ Hgmm.

The surface energy of the tubes was determined by infinite dilution inverse gas chromatography (IGC). The filler was agglomerated with water and the 250-400 μm fraction was used for the packing of the column. The dispersion component of surface tension was determined by the injection of n-alkanes at various temperatures between 160 and 300 °C, because of the high surface energy of the mineral. Only one polar probe molecule, benzene, could be eluted from the surface of the mineral between 280 and 300 °C, thus the polar component of surface tension could be determined only with large uncertainty.

The adsorption kinetics of quercetin onto the halloysite nanotubes was studied in suspension. Quercetin was dissolved in ethanol to prepare a solution of 0.03-2.00 g/dm$^3$ concentration. Halloysite was added subsequently and sonicated for 60 min, evacuated at 300 mbar pressure and then sonicated again for 15 min to remove the air from the tubes. The halloysite content of the dispersion was 10 g/dm$^3$ in each case. After predetermined adsorption times the slurry was centrifuged and the concentration of quercetin in the solution was determined by UV-VIS spectroscopy from the intensity of the adsorption peak appearing at 374 nm. The adsorption of quercetin was determined also by a dissolution method [26, 27] described more in detail elsewhere [28]. During the discussion of the results the quercetin content of the samples is presented in wt%, i.e. the amount of quercetin related to the weight of the halloysite. This unit allows the comparison of all results on the same scale including those of the adsorption experiments and the ones obtained on dry halloysite samples.

The interaction of quercetin with halloysite was studied with Fourier transform infrared spectroscopy (FTIR). Measurements were done both in transmission and in diffuse reflectance (DRIFT) mode. Potassium bromide pastilles containing ~0.4 wt% halloysite were prepared for the first technique, while dried powder was used in the second. The spectra were recorded in 16 scans by 2 $cm^{-1}$ resolution in both cases. Quercetin adsorption was followed also by X-ray photoelectron spectroscopy (XPS). The spectra were recorded using a Thermo Scientific K-Alpha (Thermo Fisher Scientific, UK) spectrometer equipped with a micro-focused, monochromatic $AlK_\alpha$ X-ray source (1486.6 eV). An X-ray beam of 400 μm size was used at 6 mA and 12 kV. The spectra were acquired in the constant analyzer energy mode with the pass energy of 200 eV for the survey. Narrow regions were collected using the snapshot acquisition mode (150 eV pass energy), enabling rapid collection of data (5 s per region). Charge compensation was achieved with the system flood gun that provides low energy electrons (~0 eV) and low energy argon ions (20 eV) from a single source. The argon partial pressure was $2x10^{-7}$ mbar in the analysis chamber. The Thermo Scientific Avantage software, version 5.948 (Thermo Fisher Scientific, UK), was used for digital acquisition and data processing. Spectral calibration was determined by using the automated calibration routine and the internal Au, Ag and Cu standards supplied with the K-Alpha system. The surface compositions (in atomic %) were determined by the consideration of the integrated peak areas of the detected atoms and the respective sensitivity factors. The fractional concentration of a particular element A was computed using **Eq. 1**

$$A\,(\%) = \frac{I_A / s_A}{\sum (I_n / s_n)} 100 \qquad (1)$$

where $I_n$ and $s_n$ are the integrated peak areas and the Scofield sensitivity factors, respectively, corrected for the analyzer transmission. The possible intercalation of quercetin into interlayer space was studied by X-ray diffraction (XRD). The patterns were recorded

using a Phillips PW 1830 equipment with $CuK_\alpha$ radiation at 40 kV and 35 mA in reflection mode.

The theoretical amount of quercetin which can be introduced into the voids within the tubes was estimated from pore volumes determined in different ways. Preliminary molecular modelling was carried out to estimate the strength of quercetin/halloysite interaction and the arrangement of the molecules on the surface of halloysite. Since accurate experimental geometry for halloysite nanotubes is not available, theoretical investigations were performed using the kaolinite clay mineral of similar structure as model system. The lattice parameters and atomic positions determined by low-temperature neutron powder diffraction by Bish [29] were used in the calculations. The Mercury [30] package was used for the construction of the crystal structures from the experimental parameters. The size of the monolayer model was ~15x25 Å and the free valences were replaced by hydrogen atoms. The geometry optimization of quercetin was carried out at the density functional theory (DFT) level using the M06-2X [31] functional and the 6-31++G** [32] basis set. Subsequently we generated 50-50 initial structures randomly placing the quercetin molecule on both sides of the crystal. Concerning the position of the quercetin molecule with respect to the surfaces in both cases the generated orientations included approximately 25 parallel and 25 perpendicular ones. The geometry optimization of the complexes were performed by molecular mechanics (MM) using the universal force field (UFF) [33] freezing all atomic positions in the crystal. The Gaussian 09 [34] package was used for the MM and DFT calculations.

## 3. Results and discussion

The results of the experiments are discussed in several sections. Halloysite characteristics will be presented first, followed by the results obtained in the study of adsorption kinetics. Interactions of the two components are discussed next followed by considerations about the possible location of quercetin on or within the halloysite. The surface structure of coated halloysite is considered subsequently including possible consequences for practice.

### *3.1. Halloysite characteristics*

The use of halloysite nanotubes both as controlled release support and as adsorbent requires their thorough characterization. Competitive interactions determine the amount of released material, the optimum and/or maximum amount of active component used for coating, and the rate of release. The surface energy of the mineral determines the strength of interaction, while its specific surface area as well as pore volume the adsorbed amount. However, halloysite nanotubes are rarely characterized in detail and many of the characteristics mentioned above are never determined. FTIR or UV-VIS spectroscopy are often used to follow the adsorption of a certain molecule [2, 11, 14], TEM to demonstrate tubular structure [2, 13], zeta potential, pH [2, 5] are determined occasionally, but specific surface area and pore volume [2] are rarely measured, and practically no attempt is made to determine surface energy.

Because of the high energy of their surface, halloysite nanotubes are expected to aggregate. These aggregates could be separated reasonably well by ultrasonic treatment. Particle size analysis of the mineral indicated an average particle size of 6.5 μm. The tubular structure of the anisotropic particles is clearly shown by TEM. The dimensions of the tubes were determined by image analysis from the micrographs recorded and they covered a wide

range. Their average length is 203 ± 119 nm, outer diameter 50 ± 23 and external diameter 15 ± 6 nm.

Besides particle characteristics, the surface area and pore structure are also very important for the intended application. According to the nitrogen adsorption measurements the specific surface area of the mineral is 57 $m^2/g$. A surface area was calculated also from the average dimensions of the tubes and 49 $m^2/g$ was obtained in this way. The good agreement of the two values indicates the accessibility of the total surface area, at least by nitrogen. BET measurements yielded the total pore volume (0.181 $cm^3/g$) and the volume of the micropores (0.023 $cm^3/g$) of halloysite as well. The volume inside the tubes was calculated also from tube geometry and a value of 0.039 $g/cm^3$ was obtained. This value is close to that of the pores and might determine the amount of the active molecules which can be adsorbed by halloysite, at least if the majority of the compound is loaded within the tubes.

Layered silicates often can accommodate quest molecules among their layers. Good examples are montmorillonites and layered double hydroxides [4, 35]. Accordingly, the theoretical possibility exists that halloysite can also adsorb quercetin within its layered structure. The layer distance of our mineral determined by XRD is 0.7 nm, somewhat smaller than that of montmorillonite which is around 1 nm. Although halloysite is regarded as a non-swelling clay, some sources claim the intercalation of urea [36, 37] and small molecular weight substances within the layers [38].

IGC yielded 278 $mJ/m^2$ for the dispersion component of surface tension and >1000 $mJ/m^2$ for its polar component. This latter number must be treated with the utmost care because of the technical difficulties involved in their determination. The composition and structure of the external and internal surfaces of halloysite is dissimilar, the internal surface is very similar to gibbsite, while the external one consists of silicon dioxide. Infinite dilution IGC measures the energy of the most active sites and the values do not give information

about the overall energy of the two surfaces. Dissolution measurements indicated an energetically heterogeneous surface [28], which allows for the preferential adsorption of active molecules on either side. Only additional experiments may decide the question and give information about the location of quercetin on or inside the halloysite tubes.

*3.2. Adsorption*

Quercetin was adsorbed onto the surface of halloysite from ethanol solution. Under such conditions adsorption is a competitive process, both the active molecule and the solvent competes for active sites on the surface of the mineral. Quercetin has multiple –OH groups which can interact with the surface, but ethanol is also expected to form strong secondary bonds or H-bridges with it. The amount of adsorbed quercetin is plotted against the concentration of the added quercetin in **Fig. 1**. The most active sites are occupied first; the amount of bonded quercetin increases linearly with the amount of added quercetin and practically all antioxidant molecules adsorb on the surface of the mineral. Adsorption continues with increasing concentration at larger quercetin amounts as well, but with a smaller slope. The change in slope indicates an energetically heterogeneous surface and possible multilayer coverage.

The time dependence, i.e. the kinetics, of adsorption is presented in **Fig. 2**. In agreement with the conclusion drawn in the previous paragraph, adsorption is fast initially and slows down later. At small solution concentrations the adsorption isotherm goes to saturation, but increases continuously at larger concentrations. This kinetics was observed above 2 wt% quercetin content, i.e. at 3, 5, 7, 10, 15 and 20 wt%. In the case of simple physisorption one would expect a simple correlation going towards saturation just like in our case at or below 2 wt% quercetin content (see **Fig. 2**). Such a behavior was observed practically by all the groups using halloysite as an adsorber for compounds [17, 18, 39-42].

However, both the concentration of the active component in the solution and the amount of halloysite in the slurry was smaller in the reported cases than in ours. Solution concentrations ranged between 0.03 and 0.3 g/dm$^3$ with the most frequent value of 0.05 g/dm$^3$ or less [17, 18, 39, 42], while halloysite content changed between 1 and 8 g/dm$^3$ with the usual value of 1 g/dm$^3$ [17, 18, 39, 42]. In our experiments the corresponding concentrations of the solutions were 0.03-2.00 g/dm$^3$ and uniformly 10 g/dm$^3$ for the suspension. Moreover, most of the kinetic studies were carried out in water solution previously. We may safely assume and the results strongly support the explanation that the considerable polarity of our active molecule, its relatively small solubility in ethanol, the large concentrations used and the energetically heterogeneous surface of halloysite lead to the observed unusual adsorption kinetics and to multilayer coverage.

*3.3. Interactions*

The adsorption isotherms presented above prove that quercetin molecules adsorb on the high energy surface of halloysite. The amount adsorbed is determined by competitive processes, by the relative strength of competing specific interactions. The competition is demonstrated well by **Fig. 3** comparing the amount of quercetin adsorbed from solution and that remaining on the surface after a dissolution process [28]. In this latter, the surface of the mineral is coated with increasing amounts of the active molecule and then the surplus, non-bonded compound is dissolved with an appropriate solvent, ethanol in this case. The comparison of the two correlations show that larger amount remains on the surface in the dissolution experiment than adsorbs from solution. In the latter case quercetin and solvent molecules compete for active sites and the adsorption of the solvent prevents that of the probe molecule. All active sites are occupied by quercetin molecules in the dissolution experiment and strong interaction with the surface prevent their dissolution and replacement

by the solvent.

Interactions are often followed by FTIR spectroscopy [17, 36, 43]. The overall DRIFT spectrum of quercetin, the neat halloysite and that of some coated nanotubes are shown in **Fig. 4**. Quite a few peaks of quercetin and the halloysite overlap with each other, but characteristic peaks can be distinguished which do not interfere. The bonds assigned to the surface (3698 $cm^{-1}$) and lattice (3629 $cm^{-1}$) –OH groups of the halloysite and the skeleton vibration of the aromatic rings of quercetin (1518 $cm^{-1}$) were used in further analysis. In **Fig. 5** the relative intensity of this latter is plotted against the amount of quercetin used for treatment. The two hydroxyl vibrations of halloysite were used as references in the evaluation. The non-linear correlation probably results from the simultaneous effect of the numerous factors (particle size, porosity, sample preparation conditions, etc.) influencing the intensity of DRIFT absorption. The two sets of data agree excellently indicating that quercetin does not intercalate among halloysite layers. In the case of intercalation, the interaction of surface –OH groups with quercetin would result in the shift of the corresponding vibration and also in a decrease of its intensity as shown by several sources [17, 36, 43]. In spite of some claims [43], lattice –OH groups are not available for interaction. Although surface hydroxyl groups are located also on the internal surface of the tubes and interact freely with any probe molecule, their number is small compared to the total number of such –OH groups and thus their interaction does not influence the position or intensity of the corresponding vibration.

The analysis of halloysite vibrations indicated the lack of intercalation, but did not give information about interactions. The spectra of halloysite samples coated with different amounts of quercetin are presented in **Fig. 6** in the range of the aromatic skeleton vibration of the probe molecule. The comparison of the spectra clearly shows that the band shifts towards larger wavenumbers with increasing coating and its intensity increases at the same

time. The shift exceeds 30 $cm^{-1}$ wavenumber indicating strong interaction of the components. The composition dependence of the shift is shown much better in **Fig. 7** in which the position of the vibration appearing at 1518 $cm^{-1}$ in the spectrum of neat quercetin is plotted against the amount of the active molecule used for treatment. The S shaped correlation shows a threshold or critical concentration and decreasing shift with increasing coating. We may safely assume that the band shifts considerably as an effect of interaction with the active sites of the highest energy, but less and less as the strength of interaction decreases and a multilayer forms. The results presented here corroborate those obtained in the adsorption and dissolution experiments indicating the existence of an energetically heterogeneous halloysite surface, strong interactions and multilayer coverage.

*3.4. Location*

Controlled release from devices containing nanotubes is based on the assumption that the probe molecules are located inside the tubes and they diffuse slowly into the surrounding medium. Unfortunately very few evidence is presented in the literature which unambiguously confirms this assumption. Several possibilities exist for the location of the probe molecule, it can be located on the external or internal surfaces, on both of them, or it can be even intercalated into the interlamellar space.

Several papers show that in spite of the fact that halloysite is a non-swelling clay, small molecules can enter the interlamellar space. Inorganic salts, alcohols, DMSO, formamide, acetamide [38] etc. were shown to intercalate into halloysite, but molecules much larger than water and compounds with benzene rigs cannot penetrate among the lamellae. The analysis of FTIR spectra indicated the absence of intercalation (**Fig. 5**). The penetration of molecules into the interlamellar space results in an increase of interlayer distance, which can be monitored by X-ray diffraction. Several XRD patterns are presented

in **Fig. 8**. The characteristic reflection of halloysite at 12° 2θ angle does not shift at all confirming our earlier conclusion about the lack of intercalation. Accordingly, quercetin must be adsorbed on either or both surfaces of the halloysite nanotubes.

Because of its large penetration depth (~10 μm), FTIR spectroscopy cannot differentiate between the external and internal surfaces of halloysite. XPS, on the other hand, has escape depth of a few nanometers (<10 nm) thus it probes only the external surface of the mineral. Apart from contaminations, halloysite does not contain carbon atoms thus the determination of the intensity of the C1s peak at 285 eV in the XPS spectrum allows us to follow the adsorption of quercetin. The carbon content of the samples is plotted against the amount of quercetin used for treatment in **Fig. 9**. The expected increase in carbon content can be clearly seen in the figure. A very similar correlation is obtained as in **Fig. 7**, but for a different reason. At small quercetin contents only the surface contamination is seen, the amount of quercetin is small and does not increase with increasing coverage. Apparently, quercetin is located inside the tubes until a critical concentration is reached, at which the tubes are saturated and the active molecules appear also on the external surface. The saturation tendency observed is a result of multilayer coverage, saturation is reached when the thickness of the layer equals or exceeds escape depth. The results and considerations presented above clearly show that quercetin does not penetrate the interlayer space, but at small coverage it is located within the tubes and then appears also on the external surface. This result also implies that surface energy is larger inside the tubes than outside that supports our conclusion about the energetically heterogeneous surface and explains the characteristics of quercetin adsorption from solution.

*3.5. Surface structure, consequences*

The final issues to be considered are the arrangement of quercetin molecules on the

surface of halloysite, critical concentrations and consequences for practice. Surfactants were shown to arrange on the surface of clays in different ways depending on their molecular structure and surface coverage [35, 44]. At small surface coverage the molecules orientate parallel to the surface, while arrange vertically at larger amounts. Quercetin is a fairly planar molecule (see **Scheme 1**) with a considerable number of evenly distributed functional groups thus we expect it to orientate parallel to the surface. Preliminary molecular modelling confirmed the assumption and yielded the arrangement shown in **Fig. 10**. Maybe not very easy to see, but quercetin is attached to the surface at several points simultaneously. During the geometry optimizations all the perpendicular structures turned to parallel position, and energetically deeper complexes were obtained if quercetin was placed on the proton-rich ($AlO_x(OH)_y$) side of the crystal. Consequently, the results of the theoretical investigations indicate that the adsorption of the quercetin molecule is favored on the $AlO_x(OH)_y$ side of the crystal inside the tubes and in a parallel position to the surface.

Characteristic concentrations can be derived from the various measurements. The amount of quercetin needed for complete coverage can be obtained from the FTIR measurements (see **Fig. 7**) and the value obtained is 4.5 wt%. XPS detects the filling of the tubes and the appearance of quercetin on the external surface of the nanotubes; the corresponding concentration is 3.5 wt%. Earlier dissolution measurements yielded the irreversibly bonded quercetin (0.8 wt%) and the maximum amount which cannot be dissolved from the surface with ethanol (4.0 wt%) [28]. Finally, the calculation of the volume occupied by quercetin from the density of the antioxidant allowed the estimation of the amount necessary to fill the pores, i.e. the voids inside the tubes and the value obtained was 4.1 wt%. The agreement of all these values is surprisingly good indicating a critical concentration of around 4.0 wt%. Below this value quercetin is located mostly inside the halloysite tubes and it is strongly bonded to the surface. As a consequence, its dissolution

or diffusion into the very apolar PE matrix is not probable, stabilization and controlled release effect cannot be expected. This conclusion was already partially confirmed by preliminary stabilization experiments [28]. Obviously, the critical concentration depends both on the guest molecule and the medium in question.

## 4. Conclusions

In order to check the possible use of halloysite nanotubes as a controlled release natural antioxidant device, the mineral was thoroughly characterized with various techniques including the determination of particle and tube morphology, specific surface area, pore size and volume, as well as surface energy. The tubular structure of individual particles was confirmed and BET measurements showed a relatively large specific surface area. The high surface energy determined by IGC predicted strong adsorption of the active molecules, quercetin, on the surface of halloysite and difficult release as a consequence. FTIR spectroscopy confirmed strong interaction, an energetically heterogeneous surface and the development of multilayer coverage at large loadings. FTIR and XRD experiments proved the complete lack of intercalation and showed that below 3.5 wt% quercetin loading most of the molecules are located within the tubes. Molecular modelling of the surface indicated the parallel orientation of quercetin molecules with the surface. Critical concentrations derived from various measurements agreed well with each other further confirming that up to about 4.0 wt% loading, quercetin is bonded very strongly to the halloysite surface. As a consequence, the dissolution of the active molecules is very difficult or impossible, especially into apolar media like PE, thus neither stabilization nor controlled release effect can be expected below that concentration.

## 5. Acknowledgements

The authors acknowledge the support of the National Scientific Research Fund of Hungary (OTKA Grant No. K 101124 and K 108934) for this project on the interactions and structure-property correlations in polymer nanocomposites. The research work has been part of the BME R+D+I project supported by the grant TÁMOP 4.2.1/B-09/1/KMR-2010-0002. The authors are indebted to Eszter Drotár for her help in the preparation of the TEM micrographs, to István Sajó for his assistance in the WAXS measurements, to Kisztina Nagyné-László and György Bosznai for the BET measurements, Enikő Földes and Erika Selmeci for their help in FTIR characterization and last, but not least to Erika Fekete and János Móczó for their support in the IGC investigation. Ildikó Erdőné Fazekas and Carmen Ramona Bende are acknowledged for their valuable contribution to sample preparation. The halloysite mineral was kindly supplied by Applied Minerals Inc. (USA). D. M. and M. K. gratefully acknowledge the computing time granted on the Hungarian HPC Infrastructure at NIIF Institute, Hungary.

## 6. References

1. Szente, L.; Szejtli, J. Highly Soluble Cyclodextrin Derivatives: Chemistry, Properties, and Trends in Development. *Adv. Drug Delivery Rev.* **1999**, *36*, 17–28.
2. Lvov, Y.; Abdullayev, E. Functional Polymer-Clay Nanotube Composites with Sustained Release of Chemical Agents. *Prog. Poly. Sci*. **2013**, *38*, 1690-1719.
3. Lvov, Y.; Shchukin, D. G.; Möhwald, H.; Price, R. R. Halloysite Clay Nanotubes for Controlled Release of Protective Agents. *ACS Nano;* **2008,** *2*, 814-820.
4. Ruiz-Hitzky, E.; Ariga, K.; Lvov, Y. *Bio-inorganic Hybrid Nanomaterials. Strategies, Syntheses, Characterization and Applications;* Wiley: Weinheim, 2008.

5. Veerabadran, N. G.; Price, R. R.; Lvov, Y. M. Clay Nanotubes for Encapsulation and Sustained Release of Drugs. *Nano*; **2007**, *2*, 115-120.
6. Byrne, R. S.; Deasy, P. B. Use of Porous Aluminosilicate Pellets for Drug Delivery. *J. Microencapsulation;* **2005,** *22*, 423-437.
7. Price, R. R.; Gaber, B. P; Lvov, Y. In-vitro Release Characteristics of Tetracycline HCl, Khellin and Nicotinamide Adenine Dineculeotide from Halloysite a cylindrical mineral. J. *Microencapsulation*; **2001**, *18*, 713-722.
8. Krejcova, K.; Rabiskova, M. Nano- and Microtubes for Drugs. *Chem. Listy*; **2008**, *102*, 35-39.
9. Fix, D.; Andreeva, D. V.; Lvov, Y. M.; Shchukin, D. G.; Moehwald, H. Application of Inhibitor-Loaded Halloysite Nanotubes in Active Anti-Corrosive Coatings. *Adv. Funct. Mater.* **2009,** *19*, 1720-1727.
10. Smith, A. W. Biofilms and Antibiotic Therapy: Is There a Role for Combating Bacterial Resistance by the Use of Novel Drug Delivery Systems?. *Adv. Drug Delivery Rev.* **2005**, *57*, 1539-1550.
11. Levis, S. R.; Deasy, P. D. Use of Coated Microtubular Halloysite for the Sustained Release of Diltiazem Hydrochloride and Propranolol Hydrochloride. *Int. J. Pharm.* **2003**, *253*, 145-157.
12. Kelly, H. M.; Deasy, P. B.; Ziaka, E.; Claffey, N. Formulation and Preliminary In Vivo Dog Studies of a Novel Drug Delivery System for the Treatment of Periodontitis. *Int. J. Pharm.* **2004**, *274*, 167-183.
13. Cornejo-Garrido, H.; Nieto-Camacho, A.; Gómez-Vidales, V.; Ramírez-Apan, M. T.; del Angel, P.; Montoya, J. A.; Dominquez-López, M.; Kibanova, D.; Cervini-Silva, J. The Anti-Inflammatory Properties of Halloysite. *J. Appl. Clay Sci.* **2012**, *57*, 10-16.

14. Ghebaur, A.; Garea, S. A.; Ivou, H. New Polymer–Halloysite Hybrid Materials - A Potential Controlled Drug Release System. *Int. J. Pharm.* **2012**, *436*, 568-573.
15. Qi, R.; Guo, R.; Shen, M.; Cao, X.; Zhang, L.; Xu, J.; Yu, J.; Shi, X. Electrospun Poly(lactic-co-glycolic acid)/Halloysite Nanotube Composite Nanofibers for Drug Encapsulation and Sustained Release. *J. Mater. Chem.* **2010**, *20*, 10622-10629.
16. Liu, P.; Zhao, M. Silver Nanoparticle Supported on Halloysite Nanotubes Catalyzed Reduction of 4-Nitrophenol (4-NP). *Appl. Surf. Sci.* **2009**, *255*, 3989-3993.
17. Xie, Y.; Qian, D.; Wu, D.; Ma, X. Magnetic Halloysite Nanotubes/Iron Oxide Composites for the Adsorption of Dyes. *Chem. Eng. J.* **2011**, *168*, 959-963.
18. Luo, P.; Zhao, Y.; Zhang, B.; Liu, J.; Yang, Y.; Liu, J. Study on the Adsorption of Neutral Red from Aqueous Solution onto Halloysite Nanotubes. *Water Res.* **2010**, *44*, 1489-1497.
19. Jinhua, W.; Xiang, Z.; Bing, Z.; Yafei, Z.; Riu, Z.; Jindun, L.; Rongfeng, C. Rapid Adsorption of Cr (VI) on Modified Halloysite Nanotubes. *Desalination*; **2010**, *259*, 22-28.
20. Brocca, D.; Arvin, E.; Mosbaek, H. Identification of Organic Compounds Migrating from Polyethylene Pipelines into Drinking Water. *Water Res.* **2002**, *36*, 3675-3680.
21. Al-Malaika, S.; Ashley, H.; Issenhuth, S.; The Antioxidant Role of α-tocopherol in Polymers. I. The Nature of Transformation Products of α-tocopherol Formed During Melt Processing of LDPE. *J. Polym. Sci.* A. **1994,** *32*, 3099-3113.
22. Al-Malaika, S.; Goodwin, C.; Issenhuth, S.; Burdick, D. The Antioxidant Role of Alpha-tocopherol in Polymers II. Melt Stabilising Effect in Polypropylene. *Polym. Degrad. Stab.* **1999**, *64*, 145-156.

23. Al-Malaika, S.; Issenhuth, S. The Antioxidant Role of Alpha-tocopherol in Polymers III. Nature of Transformation Products During Polyolefins Extrusion. *Polym. Degrad. Stab.* **1999**, *65*, 143-151.
24. Al-Malaika, S.; Issenhuth, S.; Burdick, D. The Antioxidant Role of Vitamin E in Polymers V. Separation of Stereoisomers and Characterisation of Other Oxidation Products of dl-alpha-tocopherol Formed in Polyolefins During Melt Processing. *Polym. Degrad. Stab.* **2001,** *73*, 491-503.
25. Tátraaljai, D.; Földes, E.; Pukánszky, B. Efficient Melt Stabilization of Polyethylene with Quercetin, a Flavonoid Type Natural Antioxidant. *Polym. Degrad. Stab.* **2014**, *102*, 41-48.
26. Papirer, E.; Schultz. J.; Turchi, C. Surface Properties of a Calcium Carbonate Filler Treated With Stearic Acid. *Eur. Polym J.* **1984**, *12*, 1155-1158.
27. Fekete, E.; Pukánszky, B.; Tóth, A.; Bertóti, I. Surface Modification and Characterization of Particulate Mineral Fillers. *J. Colloid Inerface Sci.* **1990**, *135*, 200-208.
28. Hári, J.; Gyürki, A.; Sárközi, M.; Földes, E.; Pukánszky, B. Competitive Interactions and Controlled Release of a Natural Antioxidant from Halloysite Nanotubes. *Submitted to J. Colloid Interface Sci.*
29. Bish, D. L. Rietveld Refinement of the Kaolinite Structure at 1.5 K. *Clays Clay Miner*. **1993**, *41*, 738-744.
30. Macrae, C. F.; Bruno, I. J.; Chisholm, J. A.; Edgington, P. R.; McCabe, P.; Pidcock, E.; Rodriguez-Monge, L.; Taylor, R.; van de Streek, J.; Wood, P. A. Mercury CSD 2.0 – New Features for the Visualization and Investigation of Crystal Structures. *J. Appl. Crystallogr.* **2008**, *41*, 466-470.

31. Zhao, Y.; Truhlar, D. G. The M06 Suite of Density Functionals for Main Group Thermochemistry, Thermochemical Kinetics, Noncovalent Interactions, Excited States, and Transition Elements: Two New Functionals and Systematic Testing of Four M06-class Functionals and 12 other Functionals. *Theor. Chem. Acc.* **2006**, *120*, 215-241.
32. Krishnan, R.; Binkley, J. S.; Seeger, R.; Pople, J. A. Self-Consistent Molecular Orbital Methods. XX. A Basis Set for Correlated Wave Functions. *J. Chem. Phys.* **1980**, *72*, 650-654.
33. Rappe, A. K.; Casewit, C. J.; Colwell, K. S.; Goddard III., W. A.; Skiff, W. M.; UFF, a Full Periodic Table Force Field For Molecular Mechanics and Molecular Dynamics Simulations. *J. Am. Chem. Soc.* **1992,** *114*, 10024-10035.
34. Gaussian 09, Revision B.01, Frisch, M. J.; Trucks, G. W.; Schlegel, H. B.; Scuseria, G. E.; Robb, M. A.; Cheeseman, J. R.; Scalmani, G.; Barone, V.; Mennucci, B.; Petersson, G. A.; Nakatsuji, H.; Caricato, M.; Li, X.; Hratchian, H. P.; Izmaylov, A. F.; Bloino, J.; Zheng, G.; Sonnenberg, J. L.; Hada, M.; Ehara, M.; Toyota, K.; Fukuda, R.; Hasegawa, J.; Ishida, M.; Nakajima, T.; Honda, Y.; Kitao, O.; Nakai, H.; Vreven, T.; Montgomery, J. A.; Peralta, J. E. Jr.; Ogliaro, F.; Bearpark, M.; Heyd, J. J.; Brothers, E.; Kudin, N.; Staroverov, V. N.; Keith, T.; Kobayashi, R.; Normand, J.; Raghavachari, K.; Rendell, A.; Burant, J. C.; Iyengar, S. S.; Tomasi, J.; Cossi, M.; Rega, N.; Millam, J. M.; Klene, M.; Knox, J. E.; Cross, J. B.; Bakken, V.; Adamo, C.; Jaramillo, J.; Gomperts, R.; Stratmann, R. E.; Yazyev, O.; Austin, A. J.; Cammi, R.; Pomelli, C.; Ochterski, J. W.; Martin, R. L.; Morokuma, K.; Zakrzewski, V. G.; Voth, G. A.; Salvador, P.; Dannenberg, J. J.; Dapprich, S.; Daniels, A. D.; Farkas, O.; Foresman, J. B.; Ortiz, J. V.; Cioslowski, J.; Fox, D. J. Gaussian, Inc., Wallingford CT, 2010.

35. Lagaly, G. Interaction of Alkylamines with Different Types of Layered Compounds. *Solid State Ionics;* **1986**, *22*, 43-51.

36. Horváth, E.; Kristóf, J.; Kurdi, R.; Makó, É.; Khunová, V. Study of Urea Intercalation into Halloysite by Thermoanalytical and Spectroscopic Techniques. *J. Therm. Anal. Chalorim.* **2011**, *105*, 53-59.

37. Nicolini, P. K.; Fukamachi, B. R. C.; Wypych, F.; Mangrich, S. A. Dehydrated Halloysite Intercalated Mechanochemically with Urea: Thermal Behavior and Structural Aspects. *J. Colloid Interface Sci.* **2009**, *338*, 474-479.

38. Joussein, E.; Petit, S.; Churchman, J.; Theng, B.; Righi, D.; Delvaux, D. Halloysite Clay Minerals - a Review. *Clay Miner.* **2005**, *40*, 383-426.

39. Liu, R.; Zhang, B.; Mei, D.; Zhang, H.; Liu, J.; Adsorption of Methyl Violet from Aqueous Solution by Halloysite Nanotubes. *Desalination;* **2011**, *268*, 111-116.

40. Nayak, P. S.; Singh, B. K. Removal of Phenol from Aqueous Solutions by Sorption on Low Cost Clay *Desalination;* **2007**, *207*, 71-79.

41. Liu, L.; Wan, Y.; Xie, Y.; Zhai, R.; Zhang, B.; Liu, J. The Removal of Dye From Aqueous Solution Using Alginate-Halloysite Nanotube Beads *Chem. Eng. J.* **2012**, *187*, 210-216.

42. Duan, J.; Liu, R.; Chen, T.; Zhang, B.; Liu, J. *Desalination;* Halloysite Nanotube-$Fe_3O_4$ Composite for Removal of Methyl Violet from Aqueous Solutions **2012**, *293*, 46-52.

43. Chang, P. R.; Xie, Y.; Wu, D.; Ma, X.; Amylose Wrapped Halloysite Nanotubes. *Carbohydr. Polym.* **2011**, *84*, 1426-1429.

44. Kádár, F.; Százdi, L.; Fekete, E.; Pukánszky, B. Surface Characteristics of Layered Silicates: Influence on the Properties of Clay/Polymer Nanocomposites. *Langmuir*, **2006**, *22*, 7848-7854.

**7. Captions**

Scheme 1 The chemical structure of quercetin.

Fig. 1 The amount of adsorbed quercetin plotted against that of the added quercetin. Symbols: (□) 0, (○) 1, (△) 2, (▽) 4, (◇) 10, (◁) 20 days.

Fig. 2 The time dependence of quercetin adsorption from ethanol solution at various quercetin concentrations. Symbols: (□) 0.3, (○) 0.7, (△) 1.0, (▽) 2.0, (◇) 3.0, (◁) 5.0 wt% quercetin related to the amount of halloysite.

Fig. 3 Effect of competitive interactions on the adsorption and dissolution of quercetin on or from the surface of halloysite. Symbol: (□) adsorption, (○) dissolution.

Fig. 4 Overall DRIFT spectra of quercetin, halloysite and nanotubes coated with various amounts of quercetin.

Fig. 5 Change in the relative intensity of the aromatic skeleton vibration of quercetin (1518 $cm^{-1}$) plotted against the amount of quercetin used for treatment. Surface and lattice –OH vibrations were used as reference bands: (●) surface, 3698 $cm^{-1}$, (○) lattice, 3629 $cm^{-1}$.

Fig. 6 Shift in the aromatic skeleton vibration of quercetin (1518 $cm^{-1}$) as an effect of interaction with the halloysite surface. Effect of surface loading.

Fig. 7 Position of the aromatic skeleton vibration of quercetin plotted against the amount of quercetin added.

Fig. 8 XRD patterns of neat halloysite and those recorded on nanotubes coated with different amounts of quercetin showing the lack of intercalation.

Fig. 9 Dependence of the carbon content of halloysite on the amount of quercetin added.

Fig. 10 Predicted arrangement of a quercetin molecule on the surface of halloysite; result of molecular modelling.

**Graphical Abstract, TOC**

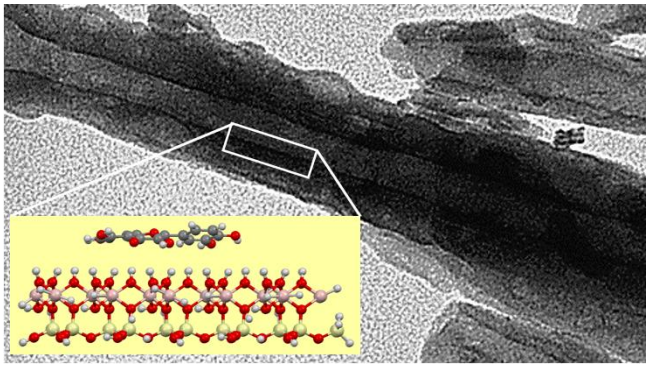

Hári, Scheme 1

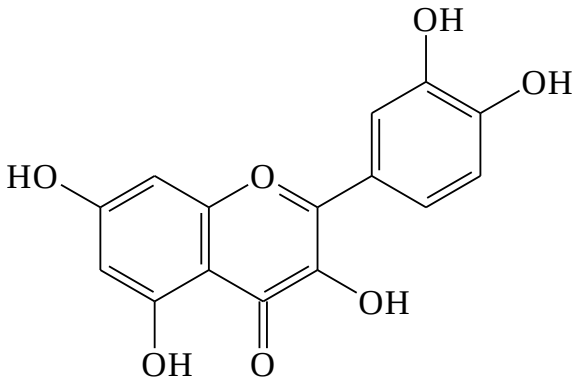

Hári, Fig. 1

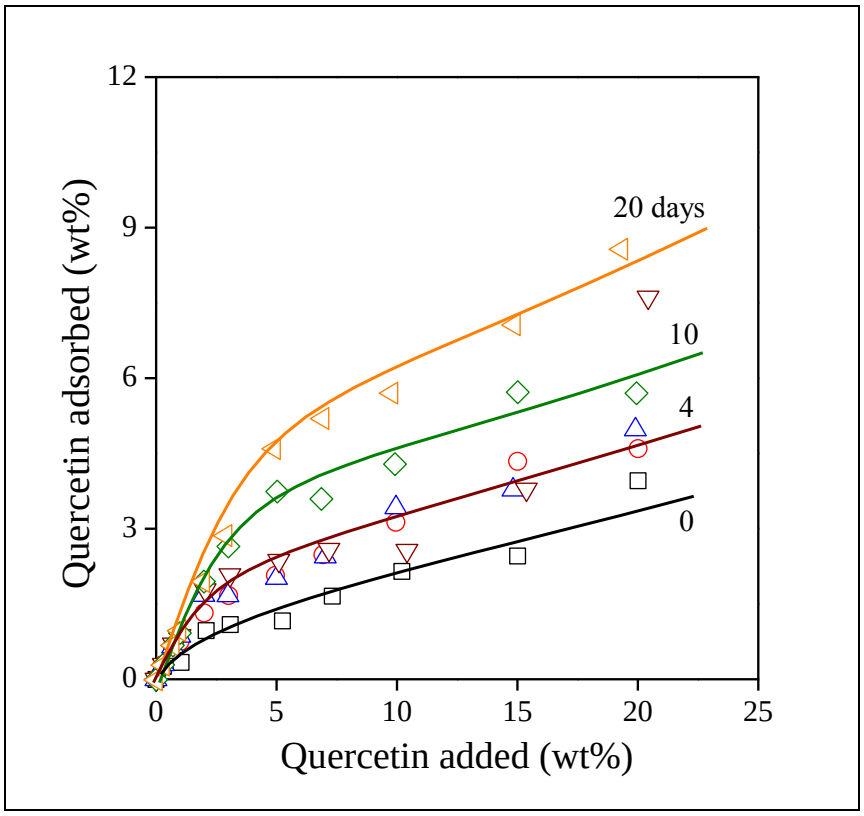
Quercetin adsorbed (wt%)
Quercetin added (wt%)
0
3
6
9
12
0
5
10
15
20
25
20 days
10
4
0

Hári, Fig. 2

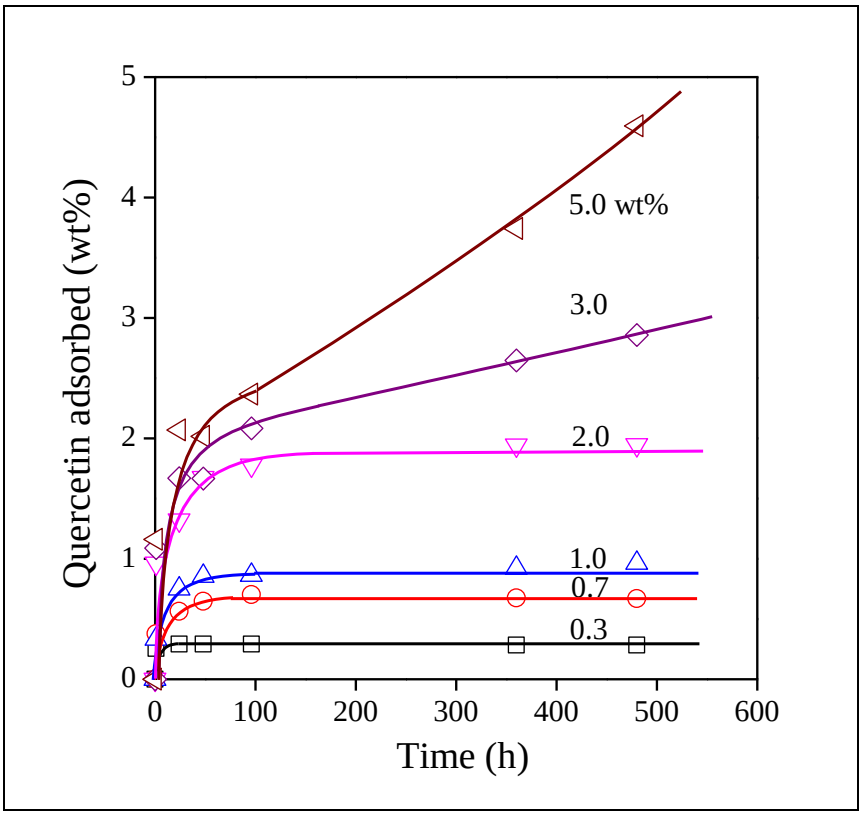
Quercetin adsorbed (wt%)
Time (h)
5.0 wt%
3.0
2.0
1.0
0.7
0.3
0
1
2
3
4
5
0
100
200
300
400
500
600

Hári, Fig. 3

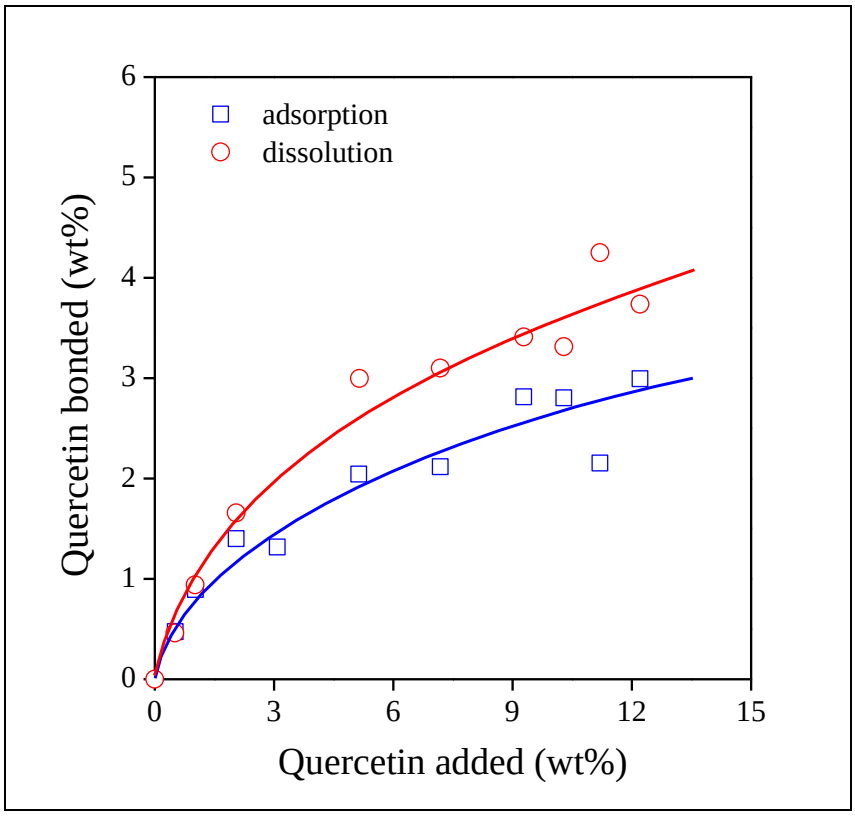
adsorption
dissolution
Quercetin bonded (wt%)
Quercetin added (wt%)
0
1
2
3
4
5
6
0
3
6
9
12
15

Hári, Fig. 4

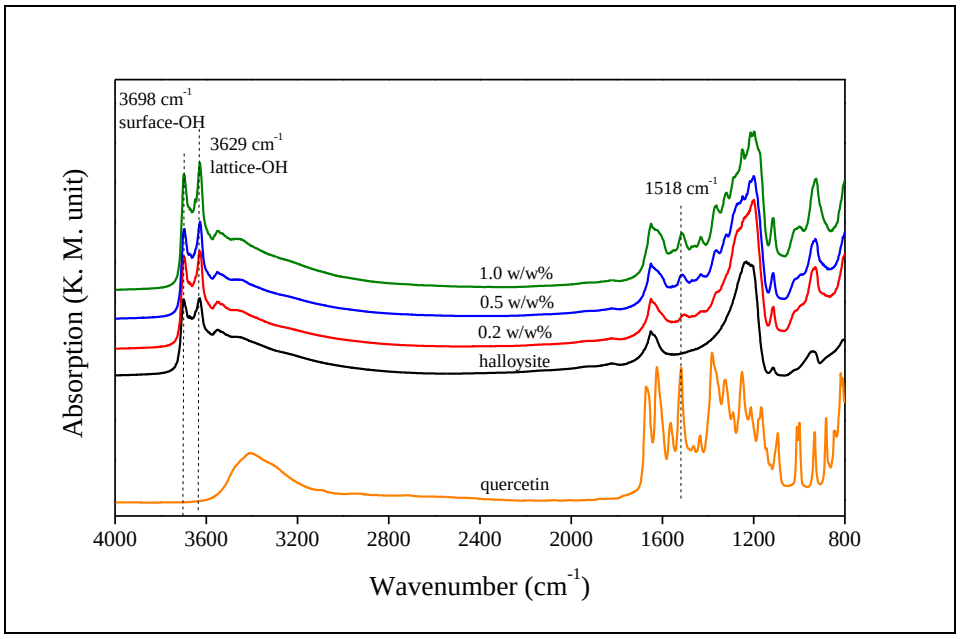
3698 cm-1
surface-OH
3629 cm-1
lattice-OH
1518 cm-1
1.0 w/w%
0.5 w/w%
0.2 w/w%
halloysite
quercetin
Absorption (K. M. unit)
4000
3600
3200
2800
2400
2000
1600
1200
800
Wavenumber (cm-1)

Hári, Fig. 5

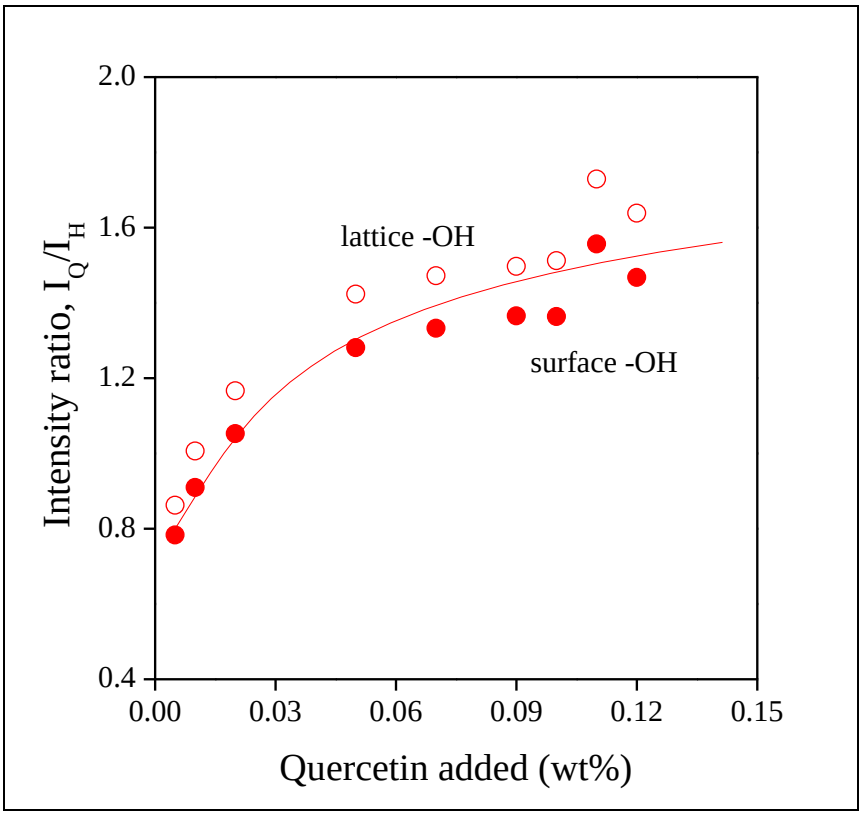
2.0
1.6
1.2
0.8
0.4
Intensity ratio, $I_Q/I_H$
lattice -OH
surface -OH
0.00
0.03
0.06
0.09
0.12
0.15
Quercetin added (wt%)

Hári, Fig. 6

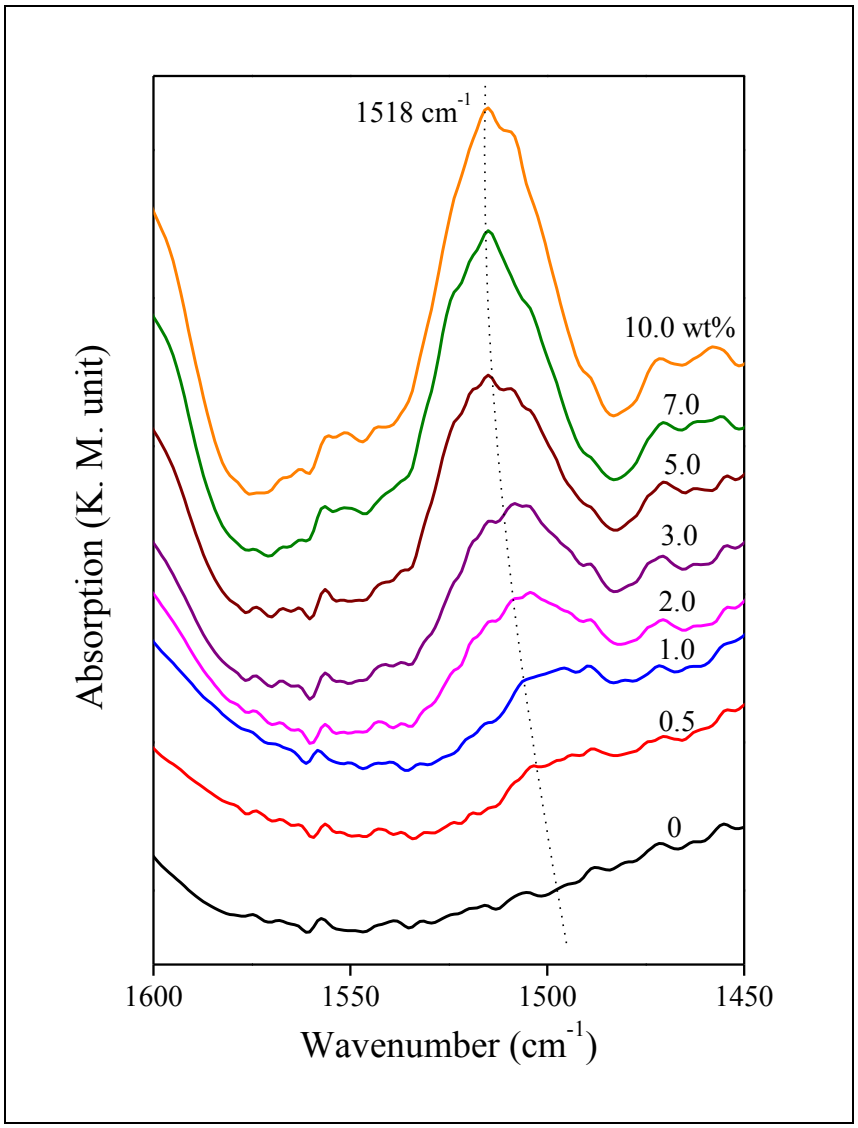
1518 cm-1
10.0 wt%
7.0
5.0
3.0
2.0
1.0
0.5
0
Absorption (K. M. unit)
1600
1550
1500
1450
Wavenumber (cm-1)

Hári, Fig. 7

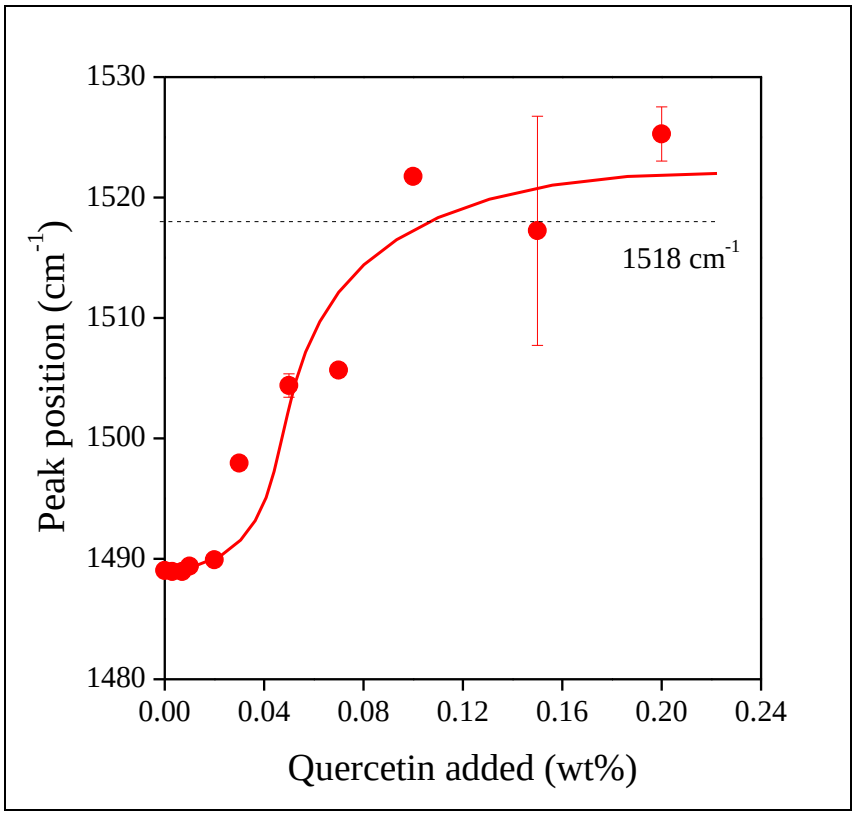
1530
1520
1510
1500
1490
1480
Peak position (cm-1)
1518 cm-1
0.00
0.04
0.08
0.12
0.16
0.20
0.24
Quercetin added (wt%)

Hári, Fig. 8

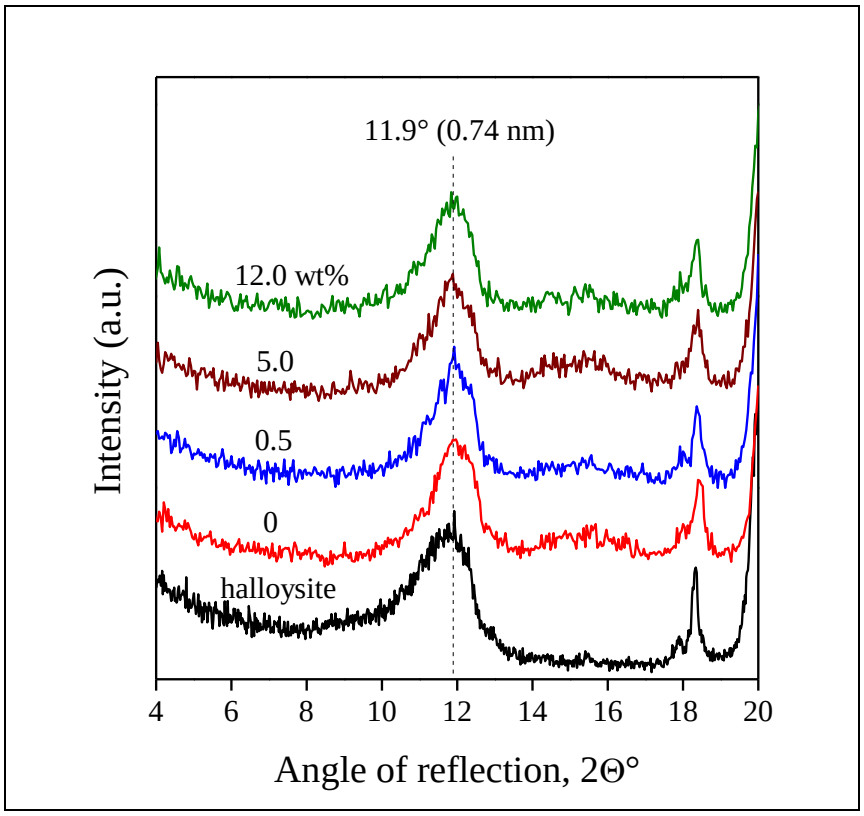
11.9° (0.74 nm)
12.0 wt%
5.0
0.5
0
halloysite
Intensity (a.u.)
4
6
8
10
12
14
16
18
20
Angle of reflection, 2Θ°

Hári, Fig. 9

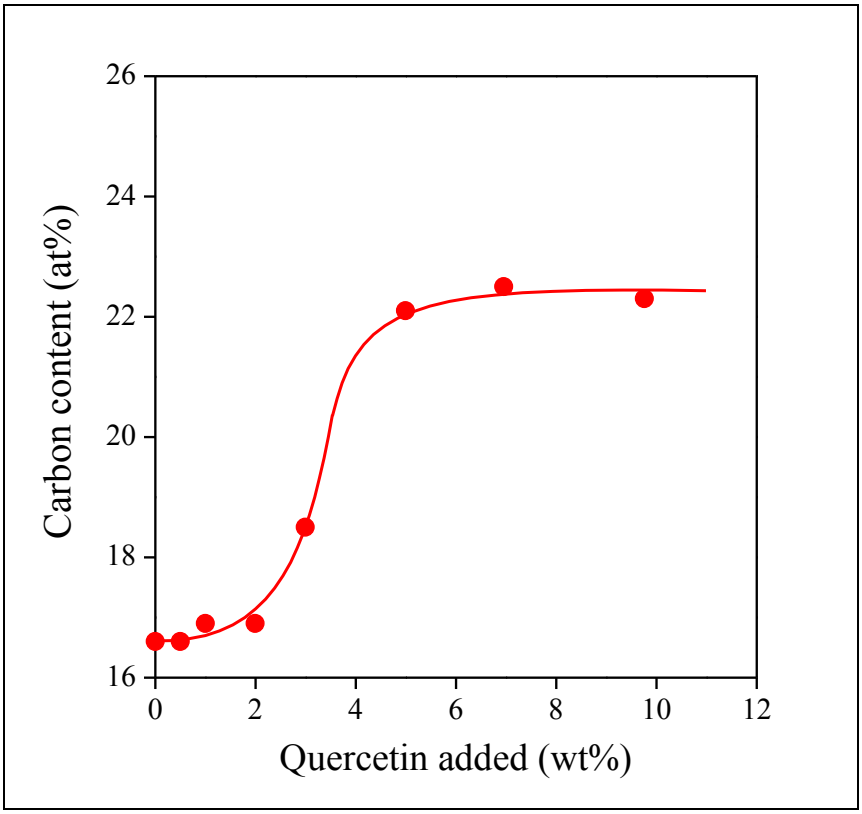
Carbon content (at%)
26
24
22
20
18
16
0
2
4
6
8
10
12
Quercetin added (wt%)

Hári, Fig. 10